Korean J. Chem. Eng., **19**(6), 992-995 (2002)

Prediction of the Solubility of 6APA in Aqueous Phase and Optimum Control Scheme for Batch Crystallization Process through pH Variation

Bahman ZareNezhad†

Chemical Engineering Department, IUST, P.O. Box 15875-4786, Tehran, Iran
(*Received 12 April 2002 • accepted 26 July 2002*)

Abstract−Solubilities of 6APA in water at different pH and temperatures are measured. A three parameter model is proposed for predicting the aqueous solubility of this amino acid. Predicted values are in good agreement with the experimental data. The model may be used for quick and accurate evaluation of the aqueous solubility of other simple ampholytes. The proposed correlation is combined with the population balance and kinetic equations for predicting the optimum pH profiles required to maintain a constant supersaturation in a batch crystallizer. The suggested policy leads to a more uniform crystal size distribution for 6APA with C.V of 23%.

Key words: 6APA Solubility, Optimum pH Profile, Batch Crystallization, Crystal Size Distribution

INTRODUCTION

6-aminopenicillanic acid (6APA) is an important intermediate in the production of synthetic penicillin. Since the published data on the aqueous solubility of 6APA in the literature are scare, a series of experiments is carried out to determine 6APA solubilities in aqueous phase at different operating conditions. These data are especially important for purification of 6APA through crystallization process by pH variations. Effect of pH changes on the solubilities of some other amino acids are reported [Zhu et al., 1990; Brown and Rousseau, 1994; Patrickios et al., 1994].

In this work, A simplified model is also developed for prediction of the effect of pH and temperature on the aqueous solubility of 6APA. The proposed solubility correlation is used in combination with crystallization model to predict the programmed pH variations required to provide a constant supersaturation. This is especially important for controlling the product crystal size distribution.

MODEL DEVELOPMENT

1. Solubility

Ampholytes are compounds capable of functioning as acids or bases according to the medium in which they are dissolved. Thus a simple ampholyte molecule HA (1 : 1 type, with $z_+=z_-$, the number of acid and base ionization constants respectively, both equal to unity) dissociates in two ways:

$$H_2A^+ + OH^- \leftrightarrow HA + H_2O \leftrightarrow H_3O^+ + A^- \quad (1)$$

Typically in aqueous solutions the ampholytes will have undergone internal ionization

$$(HA)_{solid} \leftrightarrow (^+HA^-)_{aq} \quad (2)$$

The Eq. (1) may be formulated as

$$H_2A^+ + H_2O \leftrightarrow {}^+HA^- + H_3O^+ \quad (3)$$

$$^+HA^- + H_2O \leftrightarrow H_3O^+ + A^- \quad (4)$$

Deviations from the thermodynamically ideal situation are mainly caused by the ionic strength of the solution and are relatively small for some of the aqueous solutions of amino acids including 6-APA [Tewari and Goldberg, 1988]. Thus the ionization constants can be written as:

$$K_1 = \frac{[H_3O^+][^+HA^-]}{[H_2A^+]} \quad (5)$$

$$K_2 = \frac{[H_3O^+][A^-]}{[^+HA^-]} \quad (6)$$

where $[H_2A^+]$, $[^+HA^-]$ and $[A^-]$ are the concentrations of cation, zwitterion and anion respectively.

Eq. (2) shows formation of the neutral zwitterion with its charge distribution. The zwitterion can accept a proton, as shown in Eq. (3) to form the positively charged species on the left hand side of the equation. It can also donate a proton as shown in Eq. (4) to produce a negatively charged species.

The solubility of the solute, c^*, under a given set of physical condition (i.e. pH, ionic strength and temperature), is the sum of the concentrations of these species:

$$c^* = [HA]_T = [H_2A^+] + [^+HA^-] + [A^-] \quad (7)$$

Combining Eqs. (5)-(7), gives the zwitterion concentration as:

$$[^+HA^-] = \frac{c^* K_1 / [H^+]}{1 + K_1/[H^+] + K_1K_2/[H^+]^2} \quad (8)$$

Since for a solid, the chemical potential is constant at a given temperature and pressure, the equilibrium condition can be written as:

$$\mu_{(HA)} = \mu_{(^+HA^-)} = \mu_{(^+HA^-)}^o + RT \ln a_{(^+HA^-)} = \text{constant} \quad (9)$$

Thus we have:

$$a_{(^+HA^-)} = [^+HA^-]\gamma_{(^+HA^-)} = \text{constant} \quad (10)$$

Applying ideal solution assumption to Eq. (10) at constant pres-

†To whom correspondence should be addressed.
E-mail: Zarenezhad@yahoo.com

sure and temperature gives:

$$d[^{+}HA^{-}]/dpH=0 \quad (11)$$

Considering pH=–log[H^+], Eqs. (7) and (11) are combined to give:

$$\frac{dc^*}{dpH}=-(\ln 10)[H^+]\left[\frac{dH_2A^+}{dH^+}+\frac{dA^-}{dH^+}\right] \quad (12)$$

Combination of Eq. (12) with Eqs. (5), (6) and (8) leads to the following equation:

$$\frac{d\ln c^*}{dpH}=\frac{(\ln 10)[K_1K_2(10^{2pH})-1]}{1+K_1(10^{pH})+K_1K_2(10^{2pH})} \quad (13)$$

Eq. (13) is an ordinary differential equation representing the influence of pH variations on the ampholyte solubilities in water at a given pressure and temperature.

2. Crystallization

For a perfectly mixed batch crystallizer in which crystal breakage and agglomeration are negligible, the equations obtained by moment transformation of the population balance equations [Randolph and Larson, 1971] for size independent growth rate are:

$$\frac{dm_o}{dt}=B \quad (14)$$

$$\frac{dm_{i+1}}{dt}=(i+1)m_iG \quad (15\text{-}17)$$

where $m_o(0)$ and $m_i(0)$ are zero, such that i=0, 1, 2

The mass balance in terms of the total mass deposition of the solute at constant supersaturation can be written as:

$$\frac{dc}{dt}=\frac{dc^*}{dt}=-\rho_c k_v\frac{dm_3}{dt} \quad (18)$$

Eq. (18) can be expressed in terms of pH as follows:

$$\frac{dpH}{dt}=-\rho_c k_v\frac{dm_3}{dt}\left(\frac{dc^*}{dpH}\right)^{-1} \quad (19)$$

The measured nucleation and growth kinetics of 6-APA in aqueous phase by a batch crystallizer [ZareNezhad, 2001] are correlated by power law equations in terms of influencing parameters as:

$$B=9.1\times10^4\Delta c^{3.6}M_T\varepsilon^{0.33} \quad (20)$$

$$G=4.9\times10^{-10}\Delta c^{2.4} \quad (21)$$

where Δc, M_T and ε are the supersaturation, magma density and specific power input, respectively.

The optimum pH profiles are determined by simultaneous solution of the Eqs. (13-17) and (19-21). The modified fourth order Runge-Kutta method with the time step size of 5 s is used for numerical calculations.

EXPERIMENTAL SECTION

An excess amount of 6APA crystals were added to 100 g distilled water in a jacketed glass vessel connected to a thermostatic waterbath. The solution temperature was controlled at a constant temperature with the tolerance of ±0.1 °C. Vigorous stirring was performed and the solution was left two hours to reach equilibrium. These experiments repeated seven times and the average solubility of 6-APA in distilled water at a given temperature (c_o) was recorded.

In order to determine the effect of pH variations on the solubility, a filtered saturated solution of 6APA in water at a given temperature according to above procedure was prepared. A known amount of 6APA (*m* grams) was initially added to the solution. For measuring the 6APA solubility in alkali (pH>pI), ammonia (17.5%) was dropped into the vessel and the mixture was stirred until the solids in suspension were completely disappeared. The mixture was left for an hour. When the solution remained clear, further small amount (e.g., 0.01 g) of 6APA was added to the solution.

This was done (*n* times) until the solids did not dissolve anymore. One hour was left between each of these additions.

The solution pH was then recorded by calibrated digital pH meter. Mass of added 6APA was $m+0.01(n)$.Thus the solubility of 6APA at a constant temperature and a given pH can be calculated by:

$$c^*=(c_o+m+0.01n)/(100\text{ g solvent}) \quad (22)$$

Adding a different mass (*m*) of 6APA at constant temperature enabled solubility to be obtained at different pH values.

To determine 6APA solubility in acids (pH<pI), a similar procedure was adopted using nitric acid (30%) instead of ammonia. The pH meter was recalibrated and the solubility was measured according to Eq. (22).

The nucleation and growth kinetics of 6APA in aqueous phase measured by s-plane analysis [Tavare and Garside, 1986] in a baffled agitated 3 L batch crystallizer were correlated by Eqs. (20) and (21) [ZareNezhad, 2001]. The crystal size distributions were measured by a 256 channel Coulter Counter (Model Multisizer II) interfaced with a microcomputer.

RESULTS AND DISCUSSION

Effect of pH variations on the solubilities of 6APA in water at 25 and 45 °C are shown in Fig. 1. The predicted values by Eq. (13) are also compared with experimental data in this figure.

The predicted solubility curves for 6APA appear U-shaped with a minimum at pI, which is about 4.27±0.05 in the range of 25-45 °C. This is in close agreement with value of 4.3 reported previously

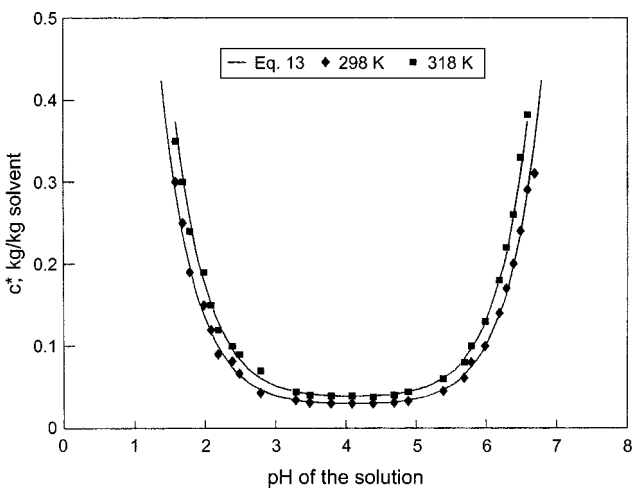

Fig. 1. Comparison of the measured and predicted solubilities of 6APA in aqueous solution at different operating conditions.

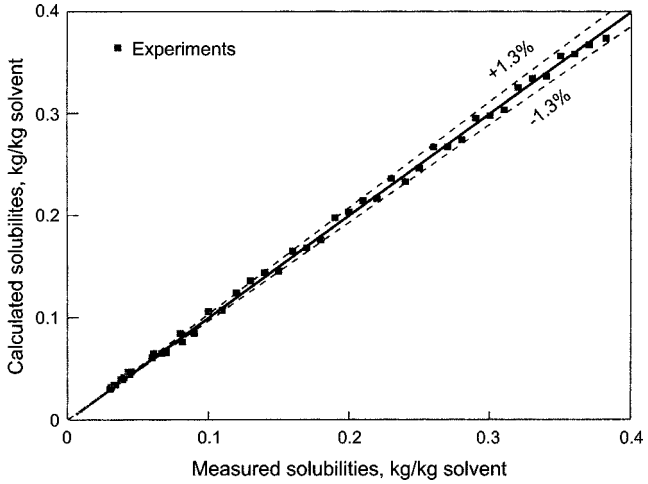

Fig. 2. Comparison of calculated aqueous solubilities of 6APA by Eq. (13) with measured values at 95% confidence limits.

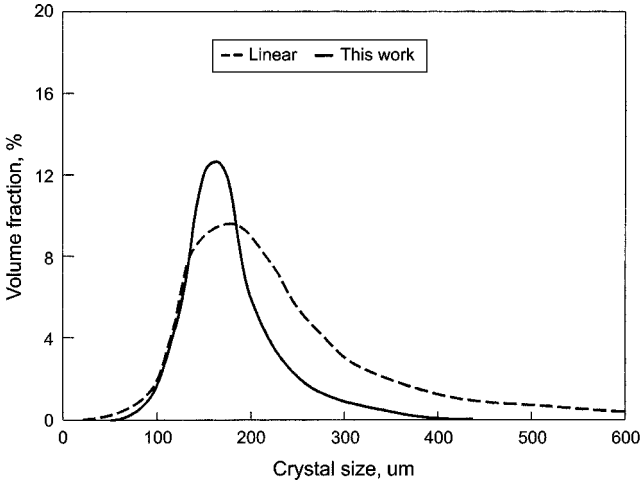

Fig. 4. Comparison of the effect of linear and optimum pH profiles on the 6APA crystal size distributions.

[ICI, 1995]. The solubility of 6APA at the isoelectric point changes slightly from 2.99 to 3.92 g/100 g solvent as the temperature increases from 25 to 45 °C. The 6APA solubility at the isoelectric condition measured at 25 °C is in good agreement with that reported by Mwangi [1994] which is about 3.02. Increased c_o leads to the upward movement of these curves. According to Fig. 1, the predicted 6APA solubilities at different pH and temperatures are in good agreement with measured data.

In Fig. 2, All the measure solubility data of 6APA are compared with predictions of Eq. (13). Two dotted lines represent the 95% confidence limits. The relative deviation between predicted and measured values for these limits is ±1.3%.

The predicted optimal pH-time curve at T of 25 °C and N of 350 Hz at different supersaturated levels are shown in Fig. 3. It can be seen that the supersaturation level is a crucial operating parameter which greatly affects the optimum pH profiles. The high supersaturation levels lead to more nuclei and resulting crystals can grow faster under the higher driving force. The solute is subsequently consumed much faster, so that the operating time is greatly shortened when the supersaturation level increases. Fig. 3 shows that as the Δc is increased from 3 to 6 kg/m^3, the solution pH should be decreased more quickly to the isoelectric value by the control system. The programmed pH variations are terminated in 202 and 38 minutes respectively after starting the operations as shown in Fig. 3.

Fig. 4 represents the size distributions of the 6APA obtained from the batch crystallization process under the two different control types after 2 hr operation. The main feature arising from this figure is the significant differences in the width of the crystal size distribution. The crystals were of a wider distribution (C.V.=37%) when the linear control scheme was employed and a narrower distribution of crystals (C.V.=23%) was obtained when the proposed optimum pH profile was applied. Since the amount of supersaturation is relatively kept constant during the operation of the suggested control policy, the final crystal size distribution is much more uniform with a lower coefficient of variation of 23%.

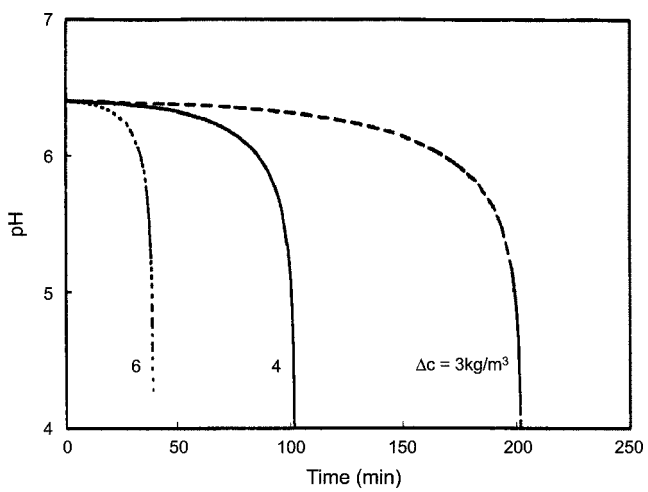

Fig. 3. Optimum pH profiles for controlled crystallization of 6APA.

CONCLUSIONS

Solubilities of 6APA in water at different temperature and pH are measured. Also a simplified model for predicting the aqueous solubility of 6APA as a function of both temperature and pH is developed. The presented model is very convenient for use with three parameters needed. Eq. (1) has been validated against 6APA solubility data obtained in this work. The optimal control scheme for the crystallization of 6APA through pH variation is established. The presented framework in this paper may be easily used for determination of the ampholyte solubilities in the aqueous phase and the programmed pH variations required to maintain a constant supersaturation in batch crystallization process. The suggested policy gives the narrowest crystal size distribution for 6APA in batch mode.

NOMENCLATURE

a : activity [kg/kg solvent]
B : nucleation rate [number/kg·s]
c^* : solubility in the solution mixture [kg/kg solvent]
c_o : solubility in the pure water [kg/kg solvent]
Δc : supersaturation [kg/m^3 solvent]

C.V. : coefficient of variation [standard deviation/mean size]
G : growth rate [m/s]
K_1 and K_2 : ionization constants [kg/kg solvent]
k_v : volume shape factor
M_T : magma density [kg/kg solvent]
m_o : zeroth moment of crystal size distribution [number/kg]
m_i : i^{th} moment of crystal size distribution [no m^{i+1}/kg]
t : time [s]
ρ_c : crystal density [kg/m^3]
μ : chemical potential [kJ/kg]
γ : activity coefficient
ε : mean specific power input [watt/kg]

REFERENCES

Brown, M. G. and Rousseau, R. W., "Effect of Sodium Hydroxide on the Solubilities of L-isoleucine, L-leucine and L-valine," *Biotechnology Progress*, **10**, 253 (1994).

ICI Technical Boultin, London, England (1995).

Mwangi, S., "Chemistry Lab. Report," UMIST, Manchester, England (1994).

Patrickios, C. S., Hertler, W. R., Abbot, N. L. and Haton, T. A., "Diblock, ABC Triblock and Random Methacrylic Polyampholytes: Synthesis by Group Transfer Polymerization and Solution Behaviour," *Macromolecules*, **27**, 115 (1993).

Randolph, A. D. and Larson, M. A., "Theory of Particulate Processes," Academic Press, New York (1971).

Tavare, N. S. and Garside, J., "Simultaneous Estimation of Crystal Nucleation and Growth Kinetics from Batch Experiments," *Chem. Eng. Res. Des.*, **64**, 109 (1986).

Tewari, Y. B. and Goldberg, R. N., "Solubility of Amino Acids in Pure Solvent Systems," *Biophys. Chem.*, **29**, 245 (1988).

ZareNezhad, B., "Determination of 6APA Crystallization Kinetics," Research Report, IUST, Tehran, Iran (2001).

Zhu, Y., Evans, L. B. and Chen, C., "Representation of Phase Equilibrium Behaviour of Antibiotics," *Biotechnol. Prog.*, **6**, 266 (1990).